Original Article

The Potential Protective Role of Hydroxytyrosol against Cypermethrin-induced Histological, Immunohistochemical and Biochemical Changes in Lung of Adult Male Albino Rats

Marwa Tharwat and Rania Said Moawad

Department of Anatomy and Embryology, Faculty of Medicine, Zagazig University, Egypt

ABSTRACT

Introduction: Cypermethrin (CYP) is a synthetic pyrethroid used as a pesticide. It induces toxicity of different organs. Hydroxytyrosol (HT) can protect against oxidant-induced toxicity and promote programmed apoptosis counteracting cellular infiltration.

Aim of the Work: The present study aimed to assess the CYP-induced histological, immunohistochemical and biochemical changes in rat lungs and to clarify the protective role of HT.

Materials and Methods: Forty adult male albino rats, their wights were (150–200 g), were used. The rats were equally distributed into four groups as follows; control group gavaged by oral route with corn oil (1 ml/kg/day), HT group gavaged by oral route with HT (50 mg/kg/day dissolved in I ml distilled water), CYP-treated group gavaged by oral route with CYP (20 mg/kg/day dissolved in I ml corn oil), and CYP+HT treated group treated orally with CYP and HT (as previous doses) for 14 days. All groups underwent histological lung examination, immunohistochemical, morphometric and biochemical analysis.

Results: This study showed that CYP caused a significant rise in MDA with a significant decline of SOD, CAT, and GSH levels. Histological changes revealed extensive cellular infiltration, thickening alveolar septum, increased angiogenesis with areas of hemorrhage, extravasation of blood, and decreased areas of ventilation in lungs of rats treated with CYP. Moreover, ultrastructural observations confirmed previous results. A noticeable improvement of the affected lung tissues was observed with HT treatment in the form of regaining of normal epithelial bronchial lining, re-inflation of alveoli and nearly intact intima of the blood vessels as well as restoration of type II pneumocyte structure.

Conclusion: HT was proved to ameliorate the CYP-induced histological, immunohistochemical and biochemical changes in rat lung, without abolishing it. This could be explained by HT's anti-inflammatory and antioxidant properties and scavenging abilities against active free radicals. These findings can be of value for future clinical applications.

INTRODUCTION

Cypermethrin (CYP) is a combined sort II synthetic pyrethroid, broad-spectrum, decomposable Insecticide and utilized in agricultural, residential, and commercial pest control applications[1]. It has a fast-acting neurotoxic effect with good contact and stomach action[2].

It is commonly used in agriculture, especially in the last two decades, because of the strong efficiency of this pesticide against a wide range of harmful organisms. The systemic effects of CYP are almost directed to the nervous system by inhibition of acetylcholinesterase[3]. The other mechanism is the oxidative stress resulting from exposure to this pesticide[4]. The relation between CYP exposure and the toxic manifestations in various organs have been studied, including hepatotoxicity, reproductive toxicity, immunotoxicity, neurotoxicity, and genotoxicity[5].

A polyphenolic antioxidant compound of the olive plant, which is Hydroxytyrosol (HT), is identified to protect cells from ROS-induced damage by scavenging free radicals in several pathological conditions[6]. It has also been reported to prevent apoptotic cell death induced by oxidative stress in various organs[7]. The exceptional antioxidant activity of HT has encouraged research in numerous fields. HT has many health characteristics including cardioprotective, antidiabetic, antioxidant, antitumoral, antimicrobial, and neuroprotective activities[8].

The current work was performed to assess lung structure by light and electron microscopes and biochemical effects of CYP insecticide on the lung of adult male rats and the protective effect of HT in alleviating the deleterious action of cypermethrin on lung structure and function.

MATERIAL AND METHOD

Chemicals

1. Cypermethrin: CYP concentration 98% liquid provided by" Jiangsu Yangnong Chemical Group Co L.T.D., China"

2. Corn oil: obtained commercially from their suppliers.

3. Hydroxytyrosol: HT was purchased from ProHealth, Inc. Carpinteria, Santa Barbara County, California, USA.

Experimental animals

Forty healthy adult male albino rats were used in the current study. Their weights were 150-200 g each and were obtained from "Animal House in the Faculty of Medicine, Zagazig University".

Experimental plan

The animals were kept under hygienic conditions with supplying them regular food and water ad-libitum and saving them in animal house in steel wire cages. The animals were kept at temperature (23°C ± 2°C) for 15 days to adapt the laboratory conditions. All rats were examined following the standard guide for the care and use of laboratory animals (IACUC approval number is ZU-IACUC/3/F/126/2020). The rats were fairly distributed into 4 main equal groups as follows:

Control group (n=10): each animal was provided (1 ml/kg/day) of corn oil (solvent of CYP) once each day for 14 days.

HT group (n=10): each animal was gavaged by oral route with HT (50 mg/kg bw) dissolved in 1 ml of distilled water, once each day for 14 days[9].

CYP-treated group (n=10): each animal was gavaged by oral route with CYP (20 mg/kg bw) dissolved in 1 ml of corn oil, once each day for 14 days[10].

CYP + HT group (n=10): each animal was gavaged by oral route with 20 mg/kg bw/d of CYP along with 50 mg/kg bw/d of HT for 14 days[9,10].

The rats in all groups were anesthetized on day 15 of the experiment by 100 mg thiopental by intraperitoneal injection, blood samples were taken, and then all rats were sacrificed The lung samples were then quickly dissected and existed carefully then immediately immersed in 10% formol saline for light microscopic examination. Another lung samples were washed with ice-cold phosphate-buffered saline (pH 7.4) and stored at −80 °C. For the biochemical assessment of oxidative stress (MDA, SOD, CAT and GSH) and the histopathological analysis, the blood and both lung tissue samples were saved.

Biochemical assessment

Fixation of lung tissues homogenates was done by a tissue homogenizer. Then centrifuged at 10,000 g at 4 °C for 20 min, and the supernatants were collected; superoxide dismutase (SOD), catalase (CAT), glutathione (GSH) activities and malondialdehyde (MDA) level were determined by a method described in previous studies[11].

Light Microscopic Examination

a- Hematoxylin and Eosin stain

The paraffin blocks of lung tissues were prepared according to standard methods[12] sections of 5 μm thickness were cut, and then stained with hematoxylin and eosin (H&E) stain for histological assessment using light microscopy (Leica ICC50W). Examination was done in "the Image analysis unit of the Department of Anatomy and Embryology, Faculty of Medicine, Zagazig University".

b-Immunohistochemical stain

For immunohistochemical analysis deparaffinized and hydrated sections were incubated for 20 min at 105 °C in Citrate buffer (pH 6.0) for antigen retrieval of the following

1- Proliferating Cell Nuclear Antigen (PCNA)

PCNA is an intranuclear polypeptide that is involved in DNA replication. Its synthesis and expression is linked to cell proliferation. Immunohistochemical staining was carried out using primary antiserum to PCNA To detect PCNA Proliferating nuclei with monoclonal antibody PC10 (Clone PC 10, DAKO A/S Denmark).

A mouse monoclonal antibody was applied in place of the primary antibody to act as a negative control. Sections from the intestne were used as a positive control. Then the slides were counterstained with haematoxylin[13].

2- Vascular Endothelial Growth Factor (VEGF)

VEGF is glycoprotein specific for angiogenesis. Its recognition was done using a specific mouse monoclonal antibody (conjugated streptavidin (Sigma). By using streptavidin-biotin peroxidase method.

Immunohistochemical control was done by omitting the primary antibody followed by incubation with the secondary antibody only to detect any nonspecific binding. Then the slides were stained with diaminobenzene (DAB) as the chromogen and counterstained with hematoxylin as previously described in literature[14]. All stained slides were examined by the light microscope (LEICA ICC50 W) and analyzed in the Image Analysis Unit of the Anatomy and Embryology Department, Zagazig University.

Morphometric analysis

After immunohistochemical staining with PCNA and VEGF, the positive area's percentage (areas stained with brown color) was calculated[15] using microscopic images captured at 400× magnification.

PCNA expression was analyzed by calculating the area percentage of PCNA positive cells. Similarly, VEGF-stained slides of all groups were studied to calculate the area percentage of VEGF positive cells.

The images are splitting into RGB stacks, then the red stack was adjusted to a threshold to mark it with a binary mask. Then the percent area relative to the field was calculated at the objective lens of 40x.

Statistical analysis

Continuous variables were represented by the mean ± SD as the data showed normal distributions (parametric). For checking the normality, the Kolmogorov-Smirnov test was used. Testing the significant differences between groups by using One-way ANOVA. Multiple comparisons between groups were performed by Post hoc Tukey's test.

At $P < 0.05$, the differences were considered significant. All statistical comparisons were two-tailed. All statistical analysis was done using Graph pad Prism software, version 5.0 (Graph Pad Software, San Diego, CA, USA)[16]

Electron Microscopic Examination

Fixation of the small pieces of lungs of all groups in 3% glutaraldehyde-formaldehyde at 4 °C for 18–24 h, rinsed in phosphate buffer, then post-fixed in 1% osmium tetroxide, then dehydrated in a series of alcohols, cleared in propylene oxide, and finally embedded in Epon epoxy resin. After that, the blocks were trimmed and sectioned with glass knives by an ultra-microtome. Semithin sections (1 mm) were stained with toluidine blue and examined on a light microscope to select the suitable area for the ultrathin sections. Ultrathin sections (70–90 nm) were cut on the same ultramicrotome and stained with uranyl acetate and lead citrate[17]. The examination of the stained sections was brought by Joel CX 100 transmission electron microscope operated at an accelerating voltage of 60 kV.

RESULTS

Control and HT groups showed no significant difference, so they considered as one group

Biochemical analysis

Evaluation of lipid peroxidation and antioxidant enzyme activities

Regarding the MDA level, there was a significant increase in the CYP-treated group (7.185± 0.3583) compared to the control group (4.380± 0.5428). While there was a significant reduction of MDA level in the CYP+HT group (6.198± 0.3755), however, its level was still higher than that of the control group (*P-value* <0.05 each) (Figure 1a).

Additionally, there was a significant decrease in the CAT level in the CYP-treated group (1.199±0.3451) than in the control group (1.731±0.3209) (*P-value* <0.05). There was a significant increase in the CAT level in the CYP+HT group (1.536±0.08120) than in the CYP-treated group (*P-value* <0.05) but without significant difference with the control group (Figure 1b).

GSH level was significantly decreased in the CYP-treated group (2.595±0.4603) than in the control group (3.582±0.3952) (*P-value* <0.05). However, in the CYP+HT group, there was a significant increase in GSH (3.081±0.2801) than that in the CYP-treated group (*P-value* <0.05) but without a significant difference from the control group (Figure 1c).

Regarding the SOD level, in the CYP-treated group, it was significantly decreased (1.292± 0.2481) compared to the control group (4.033±0.3416). While there was a significant increase in the CYP+HT group (2.448±0.2483) compared to the CYP-treated group, however, it still revealed a significant difference from the control group (*P-value* <0.05 each) (Figure 1d).

Histological Examination

Hematoxylin and Eosin stain

Examination of the control group by a light microscope revealed the normal histological architecture of the lung tissue. Several alveoli were found with thin interalveolar septa (complete 1ry septum in between alveoli) and many alveolar sacs separated by a secondary septum (Figure 2a). The epithelial lining of the alveolar walls; comprised squamous cells with flattened nuclei (pneumocytes type I) and cuboidal cells with rounded nuclei (pneumocytes type II) (Figure 2b).

In contrast, there was severe alveolar damage, in lung tissue of CYP- treated group, in the form of thickened inter-alveolar septa separating collapsed alveoli (Figures 3a,b). Dilated congested blood vessels with thickened walls, areas of exudate, erythrocytes extravasated within the lumen of alveoli were also detected. Intrabronchial cellular debris associated with RBCs appeared in most bronchioles (Figure 3a), large areas of cellular infiltration, with massive areas of hemorrhage and distorted bronchioles epithelial lining (Figure 3c).

However, lung tissue of the CYP + HT group regained inflation of most of the alveoli with obvious thin interalveolar septa, which appeared thin in some areas and mildly thickened in other areas. Bronchi regained its apparent normal epithelial lining and nearly intact intima of the blood vessels (Figure 4a). Pneumocytes type I with flat nuclei lined the wall of the alveoli and pneumocytes type II presented with rounded nuclei (Figure 4b).

Immunohistochemical analysis

1- Proliferating Cell Nuclear Antigen (PCNA)

Immunohistochemical expression of (PCNA) was expressed in the nuclei with its characteristic nuclear staining.

The mean PCNA expression showed marked variations between different groups with a higher PCNA expression in the CYP-treated group (Figure 5b) than in control (Figure 5a) and CYP+ HT groups (Figure 5c).

Using a morphometric Image J program, we measured the percentage area of brownish color (PCNA expression). A significant difference exists between the CYP-treated group compared to the control group (*P*<0.01). However, in the CYP+HT group, there was a significant reduction in PCNA expression (*P*<0.01).

Despite there was an obvious improvement by adding HT, PCNA expression was still higher in the CYP+HT group than the control (*P*<0.05) (Figure 5d).

2- Vascular Endothelial Growth Factor (VEGF)

Immunohistochemical staining with anti-VEGF antibodies localized VEGF peptide (microvascular endothelial cells) throughout the lung parenchyma.

The mean VEGF expression showed marked variations between different groups with a higher VEGF index in the

CYP-treated group (Figure 6b) than in control (Figure 6a) and CYP+HT groups (Figure 6c).

Using a morphometric Image J program, we measured the area percentage of brownish color (VEGF expression) and found a significant difference between the CYP-treated group compared to the control group ($P<0.01$). A significant decrease in VEGF expression in the CYP+HT group compared to the CYP-treated group ($P<0.01$).

Despite there was an obvious improvement by adding HT, there was still a significant difference between the CYP+HT group and the control ($P<0.05$) (Figure 6d).

Electron Microscope Examination

Ultrathin sections of the control group showed normal inter-alveolar septa, as revealed by a single capillary layer and few interstitial cells (Figure 7a). Pneumocyte type II seemed cuboidal, and their nuclei were euchromatic with short microvilli on the free cell surface. The typical appearance of several lamellar bodies in the cytoplasm was detected (Figure 7b).

In the CYP-treated group, thick inter-alveolar septa appeared with many interstitial cells. Some cells had euchromatic nuclei, and others showed apoptotic nuclei

(Figure 8a). Type II pneumocytes appeared numerous; many of which have an irregular outline with loss of apical microvilli, damaged and empty irregular lamellar bodies, which showed a disturbed architecture of many of them, scattered vacuoles in the cytoplasm and irregular nuclei (Figure 8b). A cluster of Eosinophils was noticed with the accumulation of collagen fibers in the cytoplasm (Figure 8c).

In the CYP+HT group, the inter-alveolar septa appeared thinner than those in the CYP-treated group, (Figure 9a). Restoration of type II pneumocyte structure was detected; the cells had euchromatic nuclei with full lamellar bodies, microvilli, and fewer collagen fibers in the cytoplasm (Figure 9b).

In the control group, the air–blood barrier formed by attenuated type I pneumocytes cytoplasm with a flattened nucleus, fused basal laminae, and capillary endothelial cell cytoplasm (Figure 10a). In the CYP-treated group, there was a slight swelling of the cytoplasm of type I pneumocytes (Figure 10b), but in the CYP+HT group, type I pneumocytes had regained their normal appearance (Figure 10c).
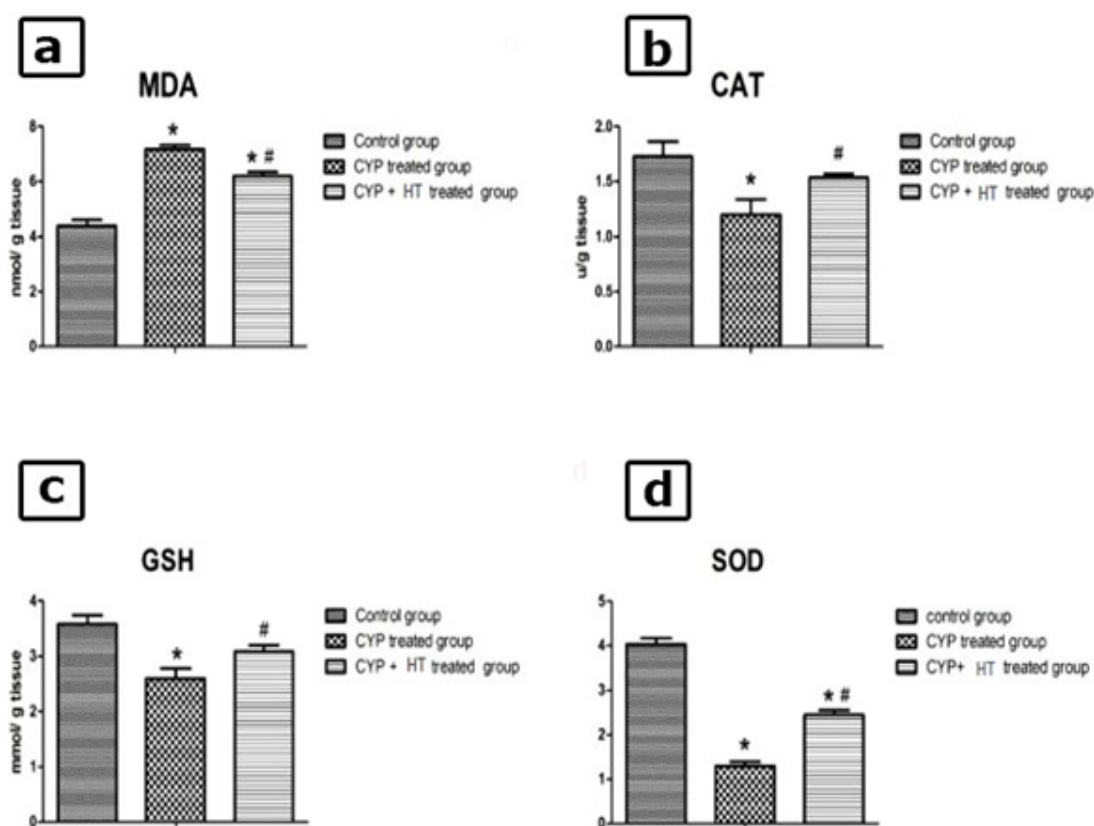

Fig. 1: Quantitative analysis of alterations in the oxidative/antioxidative markers in lung tissue of the different groups (control, CYP treated and CYP+HT)
a: MDA levels. b: CAT activity. c GSH activity. d: SOD activity. Statistical analysis carried out using one-way ANOVA, and then by post hoc Tukey's test. Values were shown as mean ± SD (n = 6).
*Significant difference compared with the control group, $P < 0.05$. #Significant difference compared with CYP treated group, $P < 0.05$.
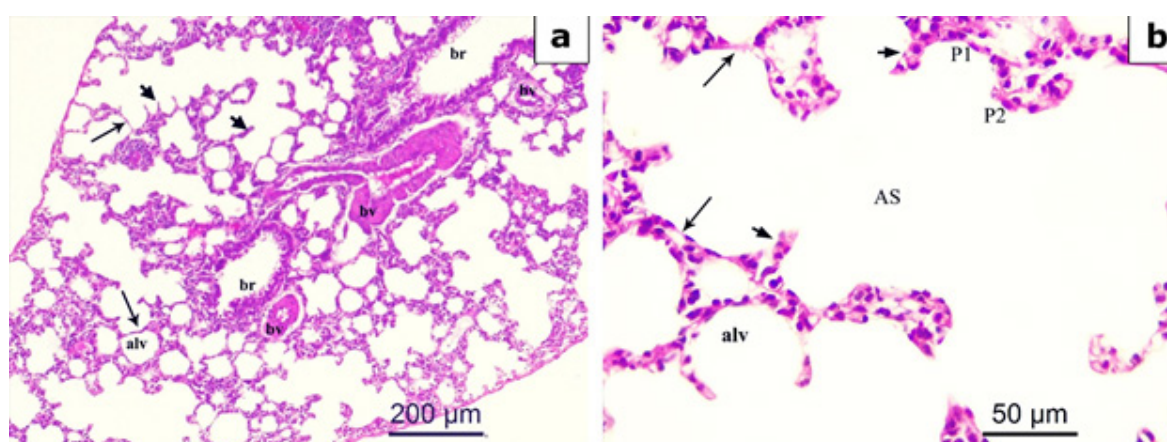
Fig. 2: Photomicrographs of the rat lung tissue of the control group showing **(a)** normal lung architecture with alveoli (alv), blood vessels (bv), and bronchioles (br). Notice the thin interalveolar septa (long thin arrow) and 2ry septum (short thick arrow). **(b)** higher magnification showing alveolar sacs (AS), flat squamous type I pneumocytes (P1) and the cuboidal type II pneumocytes (P2) lining the alveoli. Notice 1ry septa (long thin arrow) and 2ry septum (short thick arrow). Scale bar, a: 200 μmx100; b: 50 μmx400
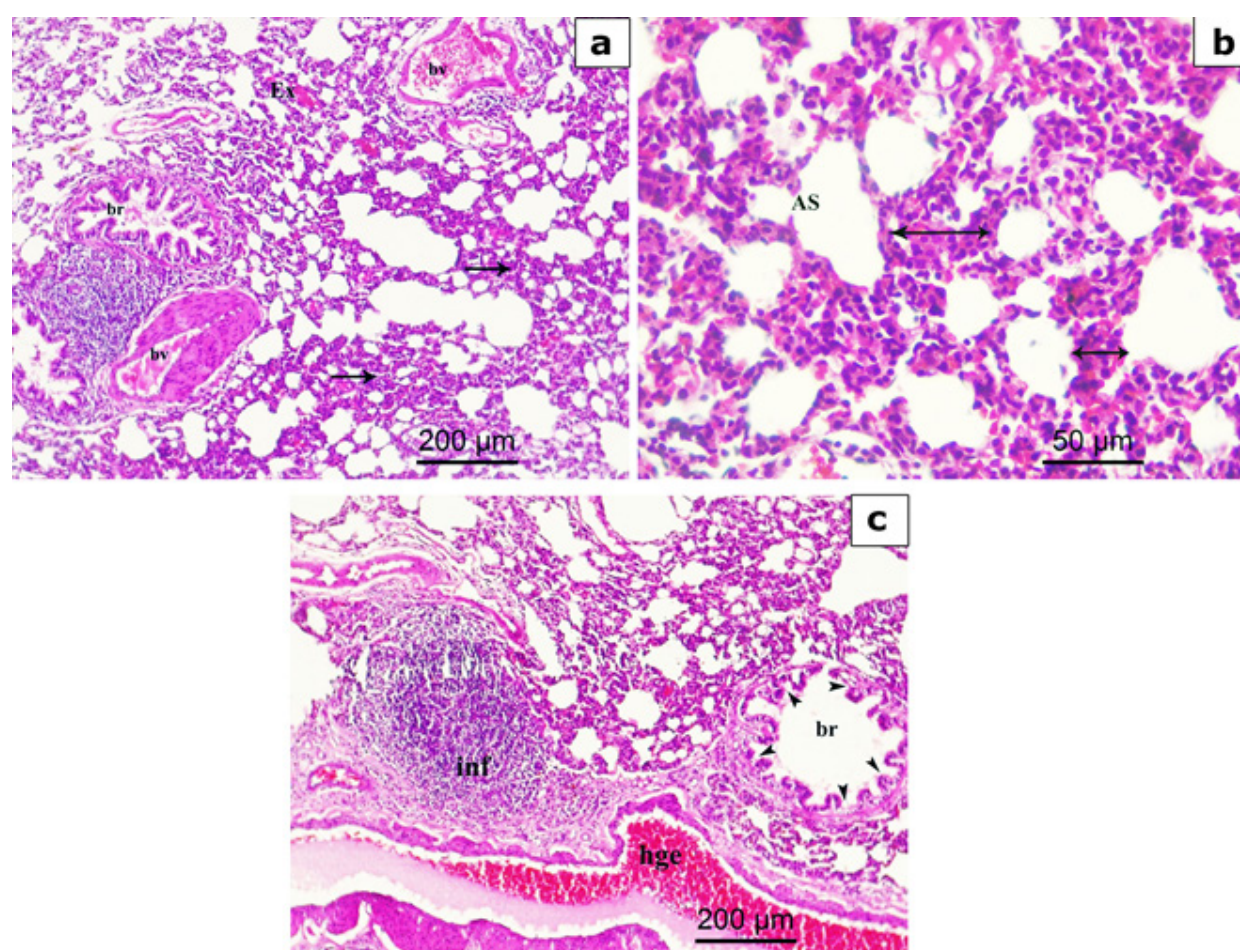

Fig. 3: Photomicrographs of the rat lung of the CYP- treated group showing **(a):** disturbed normal architecture with thick interalveolar septa (arrows). Congested and dilated blood vessels (bv), interstitial exudate (Ex) and intrabronchial cellular debris can be observed. **(b)** Higher power showing thick interalveolar septa (arrows) with narrowing of the alveolar sacs (AS). **(c)** Other image showing large cellular infiltration (inf) and disturbed mucosal lining of the bronchus (arrowheads) with massive hemorrhage (hge). Scale bar, a, c: 200 μmx100; b: 50 μmx400
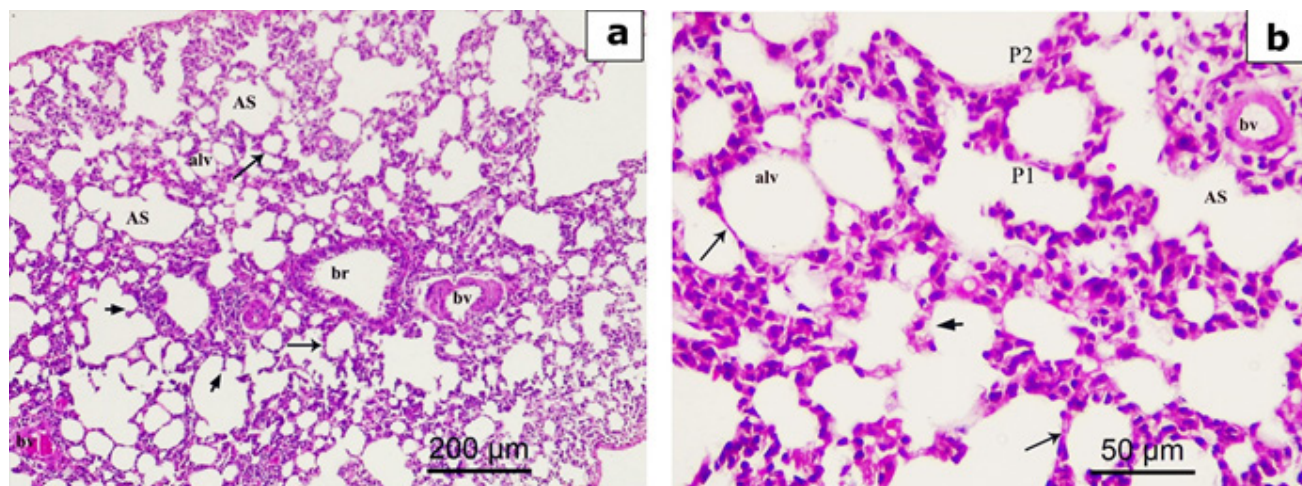
Fig. 4: Photomicrographs of the rat lung of the CYP+HT group showing **(a)** Restoring the normal architecture of the lung with bronchioles (br) has normal mucosal lining (br) as well as a nearby vessel with nearly intact intima (bv), thin 1ry interalveolar septum (long thin arrow) and 2ry interalveolar septa (short thick arrow) separating the alveolar sacs (AS) with variable thickness. **(b)** alveoli (alv), thin 1ry interalveolar septum (long thin arrow) and less marked thickness of 2ry interalveolar septa (short thick arrow) separating the alveolar sacs (AS). Flat squamous type I pneumocytes (P1) and the cuboidal type II pneumocytes (P2) lining the alveoli. Scale bar, a: 200 µmx100; b: 50 µmx400
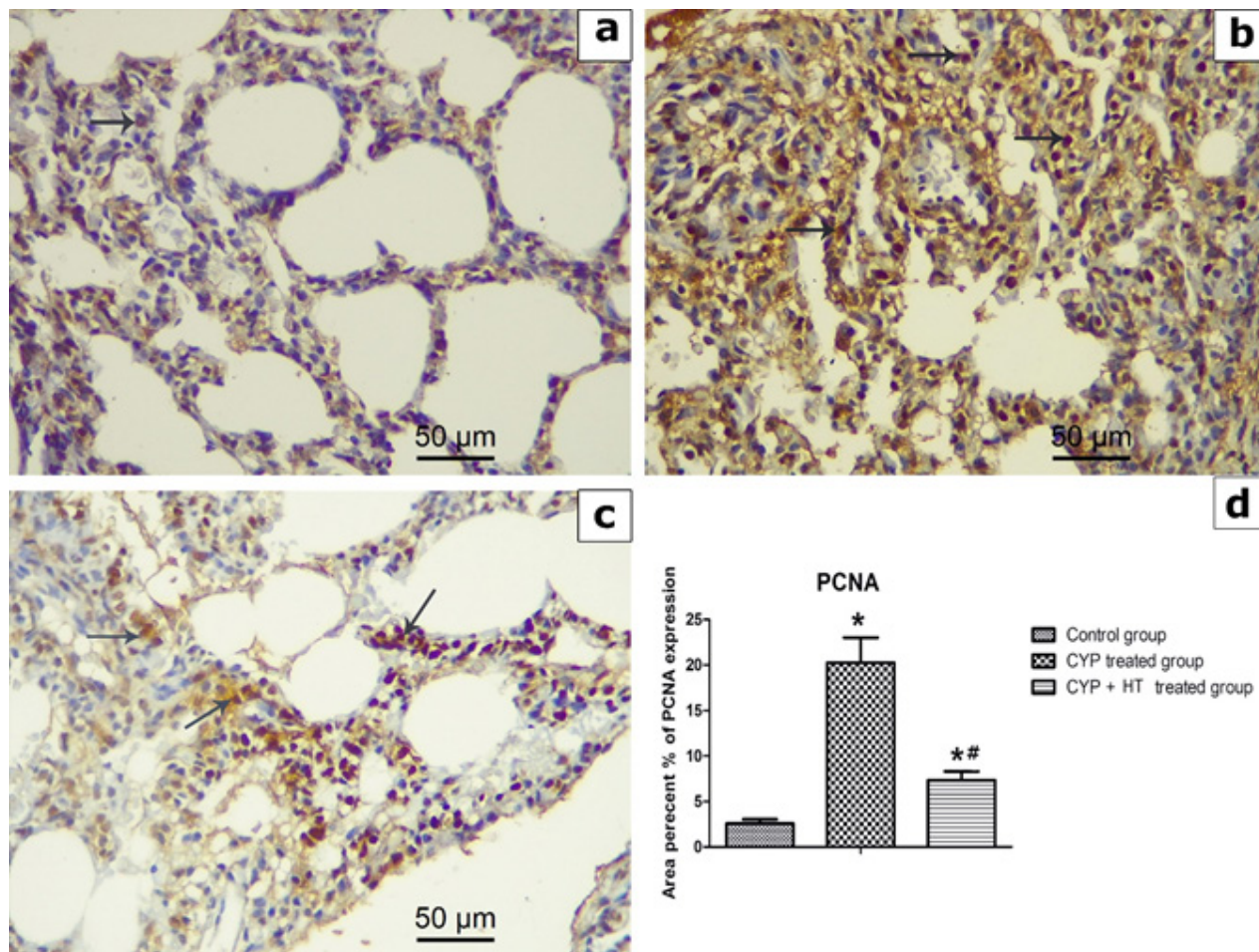

Fig. 5: Photomicrographs of PCNA immunohistochemical staining of rat lung tissue in the different groups, **a)** Control group reveals a weak reaction with few numbers of PCNA positive cells (arrow). **b)** CYP-treated group reveals strong reaction with an abundant amount of PCNA positive cells (arrows). **c)** CYP+HT group reveals moderate reaction with a minimal number of PCNA positive cells (arrows).   Scale bar, 50 µmx400 **d)** Bar chart of PCNA area percentage in different experimental groups (control, CYP-treated, and CYP+HT).
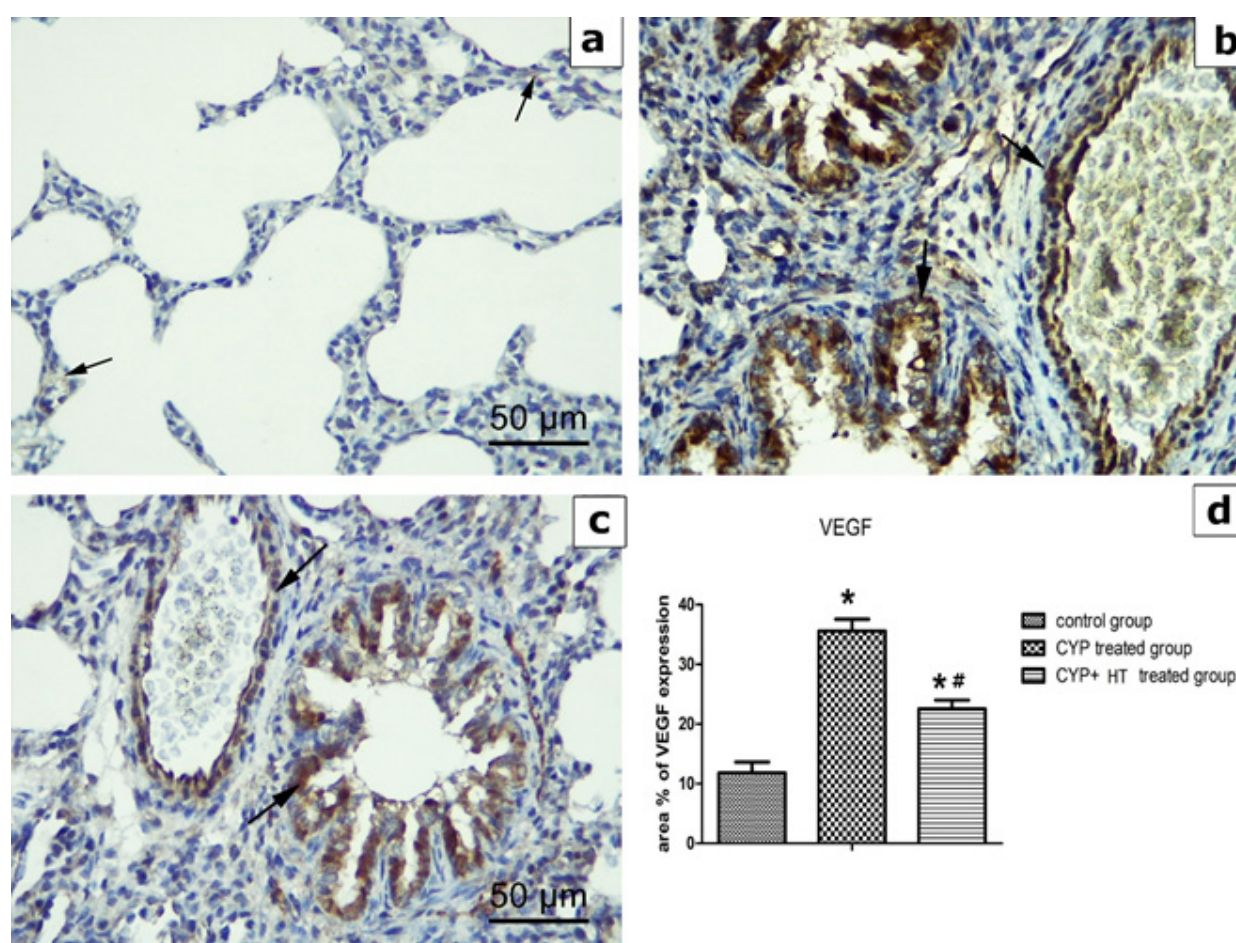* Significant difference compared to the control group.

Fig. 6: Photomicrographs of VEGF immunohistochemical staining of rat lung tissue in the different groups, **a)** Control group reveals weak reaction with few numbers of VEGF positive cells (arrows). **b)** CYP-treated group reveals strong reaction with an abundant amount of VEGF positive cells (arrows). **c)** CYP+HT group reveals moderate reaction with a minimal number of VEGF positive cells (arrows). Scale bar, 50 μmx400 **d)** Bar chart of VEGF area percentage in different experimental groups (control, CYP-treated, and CYP+HT group).
* Significant difference compared to the control group.
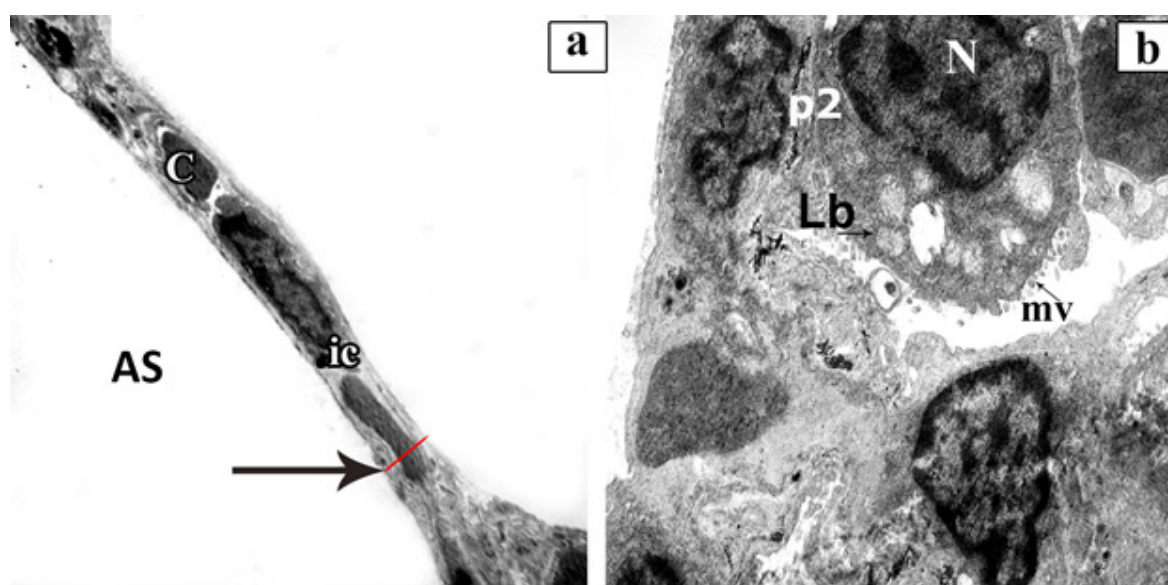# Significant difference compared to CYP-treated group.

Fig. 7: Transmission electron micrographs of a section in rat lung tissue of the control group showing **(a)** Thin (red line) interalveolar septum (arrow) separate the alveolar sacs (AS) with blood capillaries (C) on one side. Few interstitial cells can be seen (ic). **(b)** Type II pneumocyte (p2) with large euchromatic nuclei (N) and full lamellar bodies (Lb). Few apical microvilli (mv) can be noticed   a: TEM, × 6000; b: TEM,× 10000 .
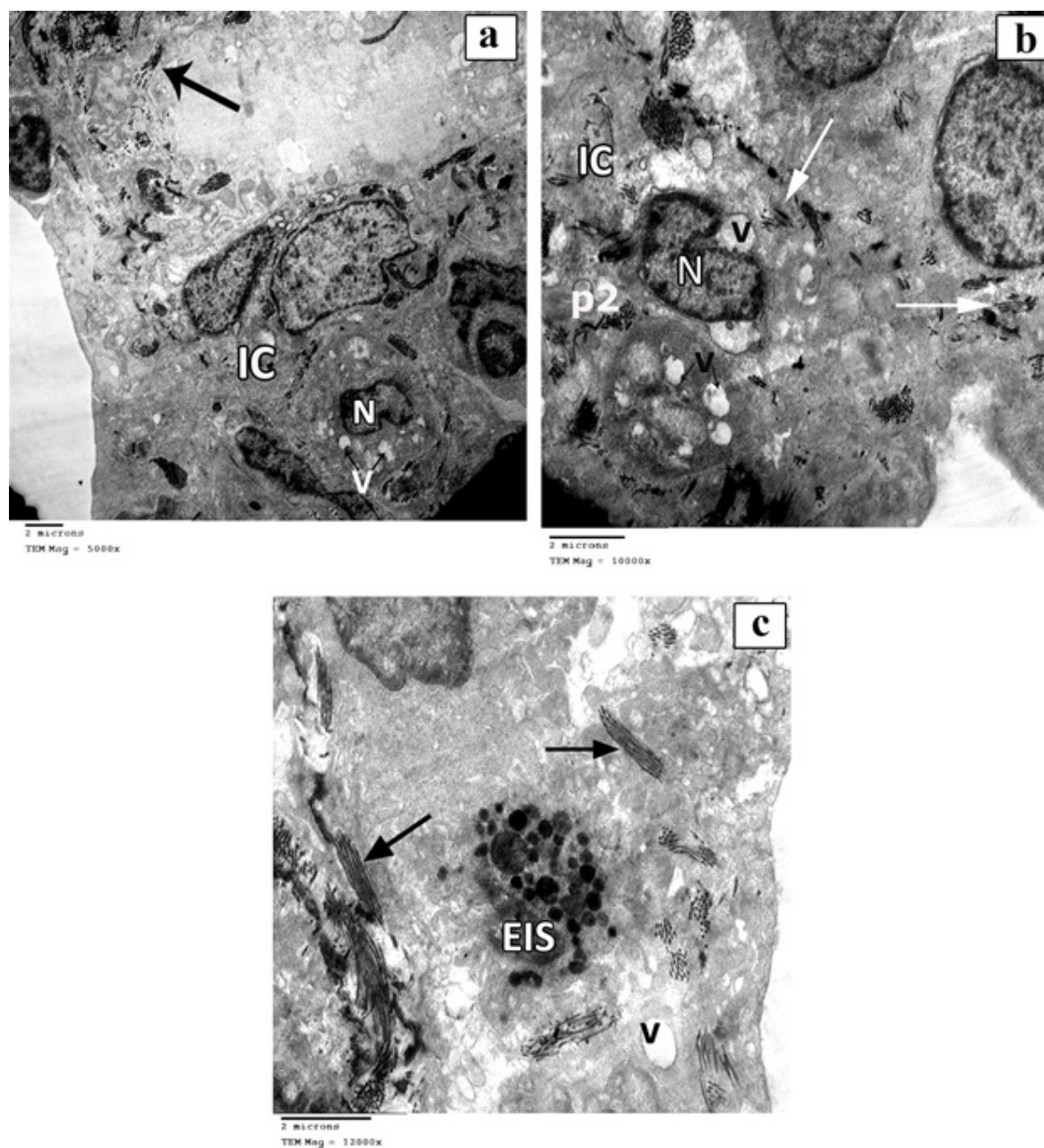
Fig. 8: Transmission electron micrographs of a section in rat lung tissue of CYP-treated group showing: **(a)** Thick interalveolar septum that has many interstitial cells (IC) with irregular nuclei (N) and numerous vacuoles (V). Many collagen fibers are also noticed (arrow). **(b)** Type II pneumocyte (p2) is detected with irregular heterochromatic nucleus (N) and numerous vacuoles (V) (empty lamellar bodies) in its cytoplasm. Many collagen fibers can be noticed (arrow). **(c)** Another section in the interstitial septum showing aggregation of eosinophils (EIS) with numerous vacuoles (V). Many collagen fibers are also seen (arrows). a: TEM, × 5000, b: TEM, × 10000   c: TEM, × 12000
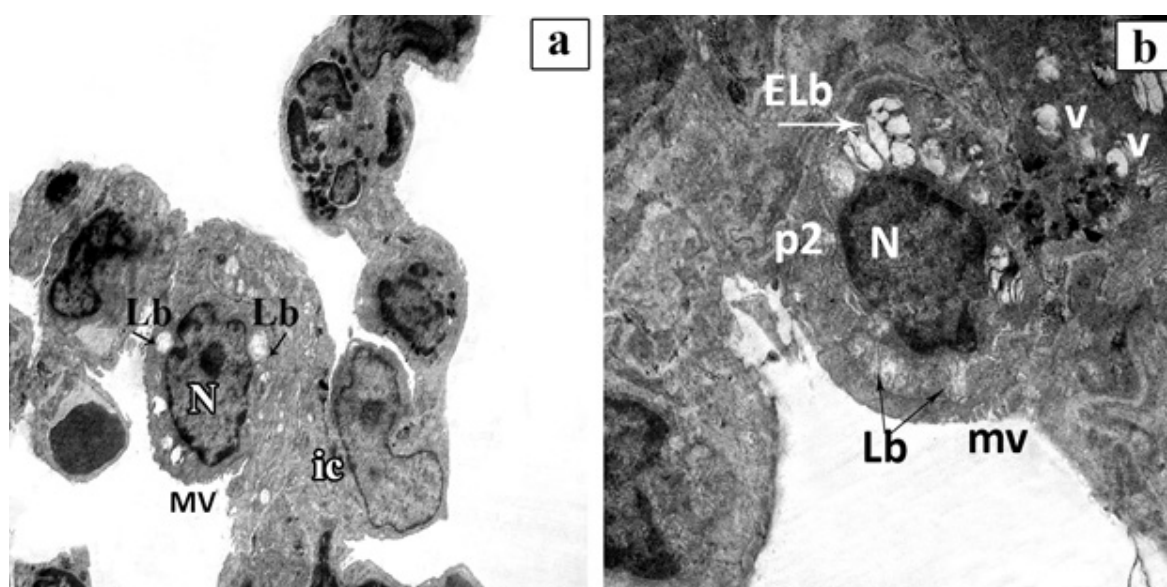
Fig. 9: Transmission electron micrographs of a section in rat lung tissue of the CYP+HT group showing **(a)** Apparently inter-alveolar septa that have few numbers of interstitial cells (ic) . Type II pneumocyte with euchromatic nuclei (N), lamellar bodies (Lb), and microvilli (MV) can be observed. **(b)** Higher magnification showing type II pneumocyte structure (p2) with euchromatic nucleus (N). Apical microvilli (mv) can be noticed. Some lamellar bodies (Lb) are full and the others are still empty (ELb). Some absorbed lamellar bodies leave empty vacuoles (V) in the cytoplasm. a: TEM, × 5000; b: TEM, × 12000

Fig. 10: Transmission electron micrographs of air–blood barrier of rat lung tissue in the different groups showing **a)** Control group reveals the air–blood barrier formed of attenuated pneumocytes type I cytoplasm (P1), fused basal laminae (arrow), and cytoplasm (C) of capillary endothelial cells (E). **b)** CYP-treated group reveals irregular air–blood barrier that has irregular swollen cytoplasm (C) of pneumocytes type I (P1) with separated basal lamina (arrow). **c)** CYP+HT group reveals nearly normal air–blood barrier. a, b, c: TEM, × 30000

DISCUSSION

In this study, the noxious effect of CYP on rat lung structure, and the protective effect of HT were investigated. Marked toxicity of the lung appeared at different biochemical, histological by light and electron microscopes as well as, immunohistochemical levels.

In this study, we used CYP pesticide due to its wide use for agricultural and household purposes, the easy accessibility of this pesticide with increased risk of suicidal, homicidal, and accidental performances, its persistence in the air and on surfaces for about 3 months, and the absence of antidote that makes it lethal upon dermal or oral exposure. All these characteristics make CYP present a challenge to public health in many countries[18,19].

Oxidative stress in rat lungs induced by CYP exposure causes a significant rise in lipid peroxidation, namely, MDA. CAT and SOD are consumed in the neutralization of CYP-induced ROS generation evidenced by the reduction in their activities. The lungs of the CYP-treated group presented ultrastructural changes with cellular damage and abnormal cellular proliferation.

Upon the addition of HT as a protective agent, CYP+HT-treated group, most of the alveoli regained their normal distended appearance, the bronchi regained also its obvious normal epithelial lining and intact intima of the blood vessels.

Improvement of biochemical parameters was detected with the decrease of oxidative stress by HT addition, which proves its strong antioxidant effect.

In this study, PCNA revealed cellular infiltration and VEGF proved the occurrence of vascular angiogenesis, in the CYP-treated group compared to the control and CYP+HT groups. The immunohistochemical study shows that mean PCNA and VEGF expression was highly significant in the CYP-treated group than in the CYP+HT one. Using morphometry for immunohistochemical sections, we found significantly fewer positive cells in the CYP+HT group compared to the CYP-treated group.

CYP exerts its effect in 2 ways; it induces oxidative stress through the generation of ROS, or by accumulation in the cell membrane disturbing its composition by its hydrophobic nature[20].

In animal models, CYP prompts mitochondrial dysfunction and oxidative stress evidenced by elevated oxidative stress markers and decreased antioxidant activities[21]. It has also been proven to increase the apoptotic index in the liver of rats, but the information is still scarce on its inflammatory effect[22].

In this study, the elevation in MDA level in the lungs indicated CYP-induced lipid peroxidation causing tissue injury. The lipophilic nature of CYP enables it to pass easily through the lipid bilayer and disturb cell integrity[23]. These observations are matched with previous studies[24] that found that CYP causes a significant elevation in the lung MDA level that in turn be considered an oxidative stress marker.

Moreover, in the current study, treatment with CYP was significantly decreased glutathione (GSH) levels in the lung tissue. Reduced GSH (an antioxidant) works by hunting ROS and xenobiotic detoxification, thus plays a vital role in cellular protection against free radicals[25]. Additionally, GSH acts as a substrate for glutathione peroxidase and glutathione-S-transferase. Oxidative stress is caused by a reduction or deficiency in antioxidants. CYP-induced GSH depletion raises the possibility of lipid peroxidation as a mechanism of CYP-induced toxicity[24]. GSH depletion also indicates cellular degeneration[26].

SOD and CAT play a primary role in the toxicity induced by mediating oxygen metabolism. The decrease in the SOD activity indicates its use in hunting the superoxide radicals. The CAT neutralizes the H_2O_2 produced by the SOD catalyzed dismutation of the superoxide anion. An increased level of superoxide radicals inhibits the activity of CAT. Additionally, the reduction in CAT activity during CYP toxicity is caused by lipid peroxidation[27]. The above-mentioned changes are due to the direct effect of CYP or induced by CYP-generated free radicals during their degradation[28]. However, another study[29] found that CYP increases SOD levels in the liver and kidney tissue. They explained the differences in results, by the difference in the CYP formulation between their study and those used in other studies. Besides, the difference in the duration and routes of exposure could be another cause of these different results.

HT reduces the previous changes caused by CYP confirming its anti-inflammatory and antioxidant properties[30]. In the present study, the protective role of HT appears through the improvement of oxidative parameters in the CYP+HT group.

The histopathological results of the CYP-treated group revealed an abnormal organization of the lung tissue in the form of marked narrowing of alveolar spaces, thickening of alveolar septa, diffuse cellular infiltrates, and inflammatory cells, blood congestion in pulmonary vessels, and thickening of interalveolar septa. These results, which support cellular infiltration resembling the early cancer stages, are concomitant with previous studies[24,31,32]. However, these results differ from those of previous studies[2,33], which revealed CYP- induced cellular necrosis and destruction of lung tissue in the form of marked dilatation in alveolar spaces and destruction of interalveolar septa.

The administration of HT with CYP proved histopathological changes and regained alveolar inflation. HT also significantly attenuated pulmonary edema and inflammatory cell infiltration into lung tissue. This is because HT has various pharmacological and biological activities, including anti-inflammatory and antioxidant effects that significantly inhibit tumor growth and angiogenesis[34]

Besides, HT can induce apoptosis, which counteracts cellular infiltration[34]

In the immunohistochemical study, we used PCNA to assess cellular infiltration and VEGF for increased angiogenesis. Many studies have been conducted to evaluate cellular proliferation and increase angiogenesis by measuring the expression of PCNA and VEGF[35–37]. PCNA is essential for DNA replication and repair, and cell growth and survival[35]. PCNA is a proliferation marker and produced by rapidly proliferating cells such as cancer cells. It degrades rapidly when these cells start the non-proliferative phase[38]. The increase in PCNA index in the CYP-treated group and its decrease with the CYP-HT group indicate that CYP causes cellular infiltration, while HT reverses such infiltration. VEGF is a cytokine that stimulates angiogenesis during embryonic development and in tumor growth[14]. It has an essential role in the control of cellular angiogenesis and controlling cellular proliferation and permeability[39]. It increases in the case of hypoxia[36]

VEGF increased in the CYP-treated group, confirming the role of CYP in damaging the lung tissue through cellular infiltration. However, VEGF decreases with apoptosis[40]. This last effect occurred upon the addition of HT.

On the ultrastructural level, lung tissue of the CYP-treated group demonstrated markedly disturbed architecture of the alveoli and lung parenchyma. These findings are concordant with the findings of a previous study[10], which confirmed that treatment with CYP at repeated oral doses of 5 and 20 mg/kg/day for 30 days produces thickening of alveolar septa in the lungs.

Ultrastructural findings in the current work showed an improvement of the alveoli of rats that were fed with HT and CYP together compared to those took CYP alone. The antioxidant effect of HT is playing a significant role in protecting cells against oxidative stress and degradation caused by free radicals[30].

Administration of HT with CYP improves histopathological changes and regains alveolar inflation and reverses cypermethrin-induced cellular infiltration. It also improves biochemical changes and oxidative stress as it has a significant antioxidant effect[41,42].

HT has several pharmacological and biological activities, including anti-inflammatory, antioxidant, and its ability to inhibit tumor growth and angiogenesis. HT also has a great role in cardiovascular protection. Another protective role of HT is to induce apoptosis, which counteracts cellular infiltration[34].

CONCLUSION

Our experimental results indicated that administration of HT counteracted most of the harmful histological lung alterations induced by CYP. Therefore, it is recommended to minimize home utilization of CYP and to perform further studies to guide human use of HT for exposed persons.

ABBREVIATIONS

CYP: Cypermethrin, **HT:** Hydroxytyrosol, **MDA:** Malondialdehyde, **SOD:** Superoxide dismutase, **CAT:** Catalase, **GSH:** Reduced glutathione.

CONFLICT OF INTERESTS

There are no conflicts of interest.

REFERENCE

1. Abdul-Hamid M, Moustafa N, Abd Alla Asran AEM, Mowafy L. Cypermethrin-induced histopathological, ultrastructural and biochemical changes in liver of albino rats: The protective role of propolis and curcumin. Beni-Suef Univ J Basic Appl Sci [Internet]. 2017;6(2):160–73. Available from: http://www.sciencedirect.com/science/article/pii/S2314853516301664

2. Nagarjuna A, Jacob Doss P. Acute oral toxicity and histopathological studies of cypermethrin in rats. Indian J Anim Res. 2009;43(4):235–40.

3. Eaton DL, Daroff RB, Autrup H, Bridges J, Buffler P, Costa LG, *et al*. Review of the Toxicology of Chlorpyrifos With an Emphasis on Human Exposure and Neurodevelopment. Crit Rev Toxicol [Internet]. 2008;38(sup2):1–125. Available from: https://doi.org/10.1080/10408440802272158

4. Idris SB, Ambali SF, Ayo JO. Cytotoxicity of chlopyrifos and cypermethrin: The ameliorative effects of antioxidants. African J Biotechnol. 2012;11(99):16461–7.

5. Mandarapu R, Prakhya BM. Exposure to cypermethrin and mancozeb alters the expression profile of THBS1, SPP1, FEZ1 and GPNMB in human peripheral blood mononuclear cells. J Immunotoxicol [Internet]. 2016;13(4):463–73. Available from: https://doi.org/10.3109/1547691X.2015.1130088

6. Goya L, Mateos R, Bravo L. Effect of the olive oil phenol hydroxytyrosol on human hepatoma HepG2 cells. Eur J Nutr [Internet]. 2007;46(2):70–8. Available from: https://doi.org/10.1007/s00394-006-0633-8

7. Pan S, Liu L, Pan H, Ma Y, Wang D, Kang K, *et al*. Protective effects of hydroxytyrosol on liver ischemia/reperfusion injury in mice. Mol Nutr Food Res [Internet]. 2013;57(7):1218–27. Available from: https://onlinelibrary.wiley.com/doi/abs/10.1002/mnfr.201300010

8. Rodríguez-Morató J, Xicota L, Fitó M, Farré M, Dierssen M, de la Torre R. Potential role of olive oil phenolic compounds in the prevention of neurodegenerative diseases. Molecules [Internet]. 2015 Mar 13;20(3):4655–80. Available from: https://pubmed.ncbi.nlm.nih.gov/25781069

9. Ristagno G, Fumagalli F, Porretta-Serapiglia C, Orrù A, Cassina C, Pesaresi M, *et al*. Hydroxytyrosol Attenuates Peripheral Neuropathy in Streptozotocin-Induced Diabetes in Rats. J Agric Food Chem [Internet]. 2012 Jun 13;60(23):5859–65. Available from: https://doi.org/10.1021/jf2049323

10. Grewal KK, Sandhu GS, Kaur R, Brar RS, Sandhu HS. Toxic impacts of cypermethrin on behavior and histology of certain tissues of albino rats. Toxicol Int [Internet]. 2010 Jul;17(2):94–8. Available from: https://pubmed.ncbi.nlm.nih.gov/21170254

11. Shi Z, Cao J, Chen J, Li S, Zhang Z, Yang B, *et al*. Butenolide induced cytotoxicity by disturbing the prooxidant–antioxidant balance, and antioxidants partly quench in human chondrocytes. Toxicol Vitr [Internet]. 2009;23(1):99–104. Available from: http://www.sciencedirect.com/science/article/pii/S0887233308002713

12. Morton J, Snider TA. Guidelines for collection and processing of lungs from aged mice for histological studies. Pathobiol Aging Age Relat Dis [Internet]. 2017 Apr 21;7(1):1313676. Available from: https://pubmed.ncbi.nlm.nih.gov/28515862

13. Elias JM, Margiotta M, Gaborc D. Sensitivity and Detection Efficiency of the Peroxidase Antiperoxidase (PAP), Avidin–Biotin Peroxidase Complex (ABC), and Peroxidase-Labeled Avidin–Biotin (LAB) Methods. Am J Clin Pathol [Internet]. 1989 Jul 1;92(1):62–7. Available from: https://doi.org/10.1093/ajcp/92.1.62

14. Fehrenbach H, Kasper M, Haase M, Schuh D, Müller M. Differential immunolocalization of VEGF in rat and human adult lung, and in experimental rat lung fibrosis: Light, fluorescence, and electron microscopy. Anat Rec. 1999;254(1):61–73.

15. Varghese F, Bukhari AB, Malhotra R, De A. IHC profiler: An open source plugin for the quantitative evaluation and automated scoring of immunohistochemistry images of human tissue samples. PLoS One. 2014;9(5).

16. GraphPad. GraphPad Statistics Guide. GraphPad Software, Inc. 2014;

17. Bozzola JJ. Conventional specimen preparation techniques for scanning electron microscopy of biological specimens. Methods Mol Biol. 2014;1117:133–50.

18. Yousef DM, El-fatah SSA, Hegazy AA, Dm Y, Ss AE, Aa H. Protective effect of ginger extract against alterations of rat thyroid structure induced by cypermethrin administration. 2019;1(1):19–25.

19. Yadav B. Cypermethrin Toxicity: A Review. J Forensic Sci Crim Investig. 2018;9(4):9–11.

20. Saxena P, Saxena AK. Cypermethrin Induced Biochemical Alterations in the Blood of Albino Rats. JJBS Jordan J Biol Sci. 2010;3(3):111–4.

21. El-Demerdash FM. Oxidative stress and hepatotoxicity induced by synthetic pyrethroids-organophosphate insecticides mixture in rat. J Environ Sci Heal Part C, Environ Carcinog & Ecotoxicol Rev [Internet]. 2011 Apr;29(2):145—158. Available from: https://doi.org/10.1080/10590501.2011.577679

22. Yavasoglu A, Sayim F, Uyanikgil Y, Turgut M, Karabay-Yavasoglu N Ülkü The Pyrethroid Cypermethrin-Induced Biochemical and Histological Alterations in Rat Liver. J Heal Sci. 2006;52(6):774–80.

23. Chrustek A, Hołyńska-Iwan I, Dziembowska I, Bogusiewicz J, Wróblewski M, Cwynar A, *et al*. Current Research on the Safety of Pyrethroids Used as Insecticides. Medicina (Kaunas) [Internet]. 2018 Aug 28;54(4):61. Available from: https://pubmed.ncbi.nlm.nih.gov/30344292

24. Arafa MH, Mohamed DA, Atteia HH. Ameliorative effect of N-acetyl cysteine on alpha-cypermethrin-induced pulmonary toxicity in male rats. Environ Toxicol. 2015 Jan;30(1):26–43.

25. Wu G, Fang Y-Z, Yang S, Lupton JR, Turner ND. Glutathione Metabolism and Its Implications for Health. J Nutr [Internet]. 2004 Mar 1;134(3):489–92. Available from: https://doi.org/10.1093/jn/134.3.489

26. Abdou H, Hussien H, Yousef MI. Deleterious effects of cypermethrin on rat liver and kidney: Protective role of sesame oil. J Environ Sci Heal Part B. 2012;47:306–14.

27. Ateşşahin A, Yilmaz S, Karahan I, Pirinçci I, Taşdemir B. The effects of vitamin E and selenium on cypermethrin-induced oxidative stress in rats ahmet. Turkish J Vet Anim Sci. 2005;29(2):385–91.

28. ERASLAN G, KANBUR M, SILICI S, ALTINORDULU S, KARABACAK M. Effecs of Cypermethrin on Some Biochemical Changes in Rats: The Protective Role of Propolis. Exp Anim. 2008;57(5):453–60.

29. Afolabi OK, Aderibigbe FA, Folarin DT, Arinola A, Wusu AD. Oxidative stress and inflammation following sub-lethal oral exposure of cypermethrin in rats: mitigating potential of epicatechin. Heliyon [Internet]. 2019 Aug 9;5(8):e02274–e02274. Available from: https://pubmed.ncbi.nlm.nih.gov/31440603

30. Crupi R, Palma E, Siracusa R, Fusco R, Gugliandolo E, Cordaro M, *et al*. Protective Effect of Hydroxytyrosol Against Oxidative Stress Induced by the Ochratoxin in Kidney Cells : in *vitro* and in *vivo* Study. 2020;7(March):1–13.

31. Iteire Afoke Kingsley, Igbigbi Patrick Sunday AAB. Histological assessment of the Effects of Pyrethroidsinsecticide Morteinon the Lungs of Adult WistarRats\n\n. IOSR J Dent Med Sci [Internet]. 2015;14(1):77–80. Available from: http://www.iosrjournals.org/iosr-jdms/papers/Vol14-issue1/Version-3/Q014137780.pdf

32. Sheikh N, Javed S, Asmatullah, Ahmad KR, Abbas T, Iqbal J. Histological changes in the lung and liver tissues in mice exposed to pyrethroid inhalation. Walailak J Sci Technol. 2014;11(10):843–9.

33. Alibraheemi A. Histopathological Alterations in Liver , Kidneys and Lungs Induced by Cypermethrin Toxicity in Albino Rats Histopathological Alterations in Liver , Kidneys and Lungs Induced by Cypermethrin Toxicity in Albino Rats. 2019;8(February):275–85.

34. Goldsmith CD, Bond DR, Jankowski H, Weidenhofer J, Stathopoulos CE, Roach PD, *et al*. The olive biophenols oleuropein and hydroxytyrosol selectively reduce proliferation, influence the cell cycle, and induce apoptosis in pancreatic cancer cells. Int J Mol Sci. 2018;19(7):1–17.

35. Lu S, Dong Z. Additive effects of a small molecular PCNA inhibitor PCNA-I1S and DNA damaging agents on growth inhibition and DNA damage in prostate and lung cancer cells. PLoS One [Internet]. 2019 Oct 10;14(10):e0223894–e0223894. Available from: https://pubmed.ncbi.nlm.nih.gov/31600334

36. Christou H, Yoshida A, Arthur V, Morita T, Kourembanas S. Increased vascular endothelial growth factor production in the lungs of rats with hypoxia-induced pulmonary hypertension. Am J Respir Cell Mol Biol. 1998;18(6):768–76.

37. Maniscalco WM, Watkins RH, Finkelstein JN, Campbell MH. Vascular endothelial growth factor mRNA increases in alveolar epithelial cells during recovery from oxygen injury. Am J Respir Cell Mol Biol. 1995;13(4):377–86.

38. Kamaraj S, Ramakrishnan G, Anandakumar P, Jagan S, Devaki T. Antioxidant and anticancer efficacy of hesperidin in benzo(a)pyrene induced lung carcinogenesis in mice. Invest New Drugs. 2009;27(3):214–22.

39. Nieves BJ, D'Amore PA, Bryan BA. The function of vascular endothelial growth factor. BioFactors. 2009;35(4):332–7.

40. Abadie Y, Bregeon F, Papazian L, Lange F, Chailley-Heu B, Thomas P, *et al*. Decreased VEGF concentration in lung tissue and vascular injury during ARDS. Eur Respir J. 2005;25(1):139–46.

41. Rietjens SJ, Bast A, De Vente J, Haenen GRMM. The olive oil antioxidant hydroxytyrosol efficiently protects against the oxidative stress-induced impairment of the NO• response of isolated rat aorta. Am J Physiol - Hear Circ Physiol. 2007;292(4):1931–6.

42. Loru D, Incani A, Deiana M, Corona G, Atzeri A, Melis MP, *et al*. Protective effect of hydroxytyrosol and tyrosol against oxidative stress in kidney cells. Toxicol Ind Health [Internet]. 2009;25(4–5):301–10. Available from: https://doi.org/10.1177/0748233709103028

الملخص العربى

الدور الوقائي المحتمل للهيدروكسي تيروسول ضد التغيرات النسيجية والنسيجية المناعية والكيميائية الحيوية التي يسببها سايبرمثرين في رئة ذكور الجرذان البيضاء البالغة

مروة ثروت عبد الفتاح؛ رانيا سعيد معوض

قسم التشريح والأجنة ـ كلية الطب ـ جامعة الزقازيق

الخلفية: سايبرمثرين عبارة عن بيرثرويد اصطناعي يستخدم كمبيد للآفات و يسبب تسمم الأعضاء المختلفة. يمكن أن يحمي الهيدروكسى تيروكسى من السمية التي تسببها الأكسدة ويعزز موت الخلايا المبرمج الذي يقاوم التسلل الخلوي.

الهدف من العمل: تهدف الدراسة الحالية إلى فحص التغيرات النسيجية والهيستوكيميائية المناعية والكيميائية الحيوية التي يسببها السايبرمثرين في رئتي الجرذان البيضاء وتوضيح الدور الوقائي المضاد للهيدروكسى تيروسول.

المواد والطرق: استخدم أربعين من ذكور الجرذان البيضاء البالغة ، تراوحت أوزانها بين ١٥٠-٢٠٠ جم. قسمت الفئران بالتساوي إلى أربع مجموعات على النحو التالي ؛ المجموعة الضابطة أعطيت زيت الذرة (١ مل / كجم / يوم) عن طريق الفم ، مجموعة الهيدروكسى تيروسول أعطيت عن طريق الفم الهيدروكسى تيروسول (٥٠ مجم / كجم / يوم مذاب في ١ مل من الماء المقطر) ، المجموعة المعالجة بالسايبرمثرين عن طريق الفم السايبرمثرين (٢٠ مجم / كجم / يوم مذاب في I ml زيت ذرة) ، ومجموعة السايبرمثرين و الهيدروكسى تيروسول المعالجة بالفم باستخدام السايبرمثرين و الهيدروكسى تيروسول (كالجرعات السابقة). بعد ١٤ يوم خضعت جميع المجموعات للفحص النسيجي المجهري للرئة وكذلك دراسة الهيستوكيميائية المناعية ومورفومترية وللتحليل البيوكيميائي.

النتائج: أظهرت هذه الدراسة أن السايبرمثرين تسبب في ارتفاع كبير في MDA مع انخفاض كبير في مستويات SOD و CAT و GSH. كشفت التغيرات النسيجية المحدثة بالسايبرميثرين عن تسلل خلوي وسماكة للحاجز السنخي ، وزيادة تكوين الأوعية مع تسرب كرات دموية ، وقلت مساحة الاسناخ الرئوية في رئتي الجرذان المعالجة بالسايبرمثرين. علاوة على ذلك ، الدراسة النسيجية باستخدام الميكروسكوب الالكتروني أكدت نفس النتائج. شوهد تحسن واضح في أنسجة الرئة المصابة بعد اعطاء علاج الهيدروكسى تيروسول في شكل استعادة بطانة الشعب الهوائية ، ورجوع حجم الحويصلات الهوائية لوضعها الطبيعي ، و بدت البطانة الداخلية للأوعية الدموية سليمة تقريبًا وكذلك استعادت الخلايا الرئوية من النوع الثاني تركيبها الطبيعي.

الاستنتاج: ثبت ان الهيدروكسى تيروسول له تأثير وقائي ضد التغيرات النسيجية والهيستوكيميائية المناعية والكيميائية الحيوية التي سببها السايبرمثرين في رئة الجرذان البيضاء. وقد يعزي ذلك إلى خصائصه المضادة للالتهابات ومضادات الأكسدة وقدرته علي إزالة الشوارد الحرة النشطة. لذلك فإن إضافة الهيدروكسي تيروسول يمكن أن يضاد التغييرات الحادثة في الرئتين والناتجة عن السايبرمثرين. وهذه النتائج قد تحمل قيمة وتؤخذ توصياتها في التطبيق الإكلينيكي .